

Defect-assisted relaxation in quantum dots at low temperature

Darrell F. Schroeter* and David J. Griffiths
Department of Physics, Reed College, Portland, Oregon 97202

Peter C. Sercel
Department of Physics and Materials Science Institute, University of Oregon, Eugene, Oregon 97403
 (Received 13 October 1995; revised manuscript received 14 March 1996)

A model for electron relaxation in a quantum dot, including a nonradiative pathway through a point defect, is presented, using time-dependent perturbation theory. The results obtained here extend previous work [Phys. Rev. B **51**, 14 532 (1995)] to the experimentally relevant low-temperature regime. It is found that relaxation through defects may circumvent the phonon bottleneck predicted for ideal nanometer-scale quantum dot structures even at low temperatures. [S0163-1829(96)06828-2]

For nanometer scale quantum dots, the separation between adjacent electron energy levels may exceed the LO phonon energy. In this regime, single phonon emission cannot account for electron relaxation between adjacent energy levels. The alternatives, multiple phonon and radiative processes, occur much more slowly, resulting in prolonged lifetimes for electrons in excited states of the quantum dot.^{1,2} This effect is known as the “phonon bottleneck.” While this effect appears to stand on firm theoretical ground, it has not been observed in recent experiments on high-quality quantum dots.³

Several models have been proposed to solve the “phonon bottleneck” problem. Inoshita and Sakaki⁴ have shown that processes involving one LO phonon and one LA phonon can provide a pathway for rapid relaxation between electronic states separated by $\hbar\omega_{LO} \pm \hbar\omega_{LA}$, however, this process is inoperative for quantum dots where the intraband spacing is substantially greater than the LO phonon energy. Other investigators have examined the role of Auger-like processes in overcoming the phonon bottleneck.^{5,6} This type of mechanism could allow for relaxation on picosecond time scales.

An alternate model wherein electrons thermalize by coupling to nearby traps or interfacial defects has been proposed by Sercel.⁷ In this model, relaxation occurs by the following sequential process: an electron makes a transition from the quantum dot to the defect, the defect relaxes by multiphonon emission, and the electron makes a second transition to a lower-lying energy level of the quantum dot. The defect functions as a sort of “elevator” carrying the electron from the upper level in the quantum dot to the lower level, providing a channel for nonradiative intraband carrier relaxation. Sercel’s analysis is based upon a semiclassical approximation for the lattice, strictly valid only when the thermal energy in the system is greater than the height of the activation barrier for a dot-defect transition. The conclusion of Sercel’s study was that defect-assisted relaxation could play a role in breaking the phonon bottleneck effect in nanometer-scale quantum dots. However, the majority of experiments performed on quantum dots are carried out at cryogenic temperatures where the semiclassical approximation fails.

In the present paper the low-temperature rates are calculated fully quantum mechanically, and it is found that the defect-assisted relaxation rates may remain large even at low temperatures. The analysis shows that electron relaxation via the defect-coupling channel circumvents the phonon-bottleneck effect in qualitative agreement with experiments reported in Ref. 3.

To conform with the analysis of Sercel,⁷ we consider a model spherical $\text{In}_{0.5}\text{Ga}_{0.5}\text{As}/\text{GaAs}$ quantum dot with a radius of 5 nm, and a point defect located within the GaAs matrix. At this radius, the dot has only two bound conduction states, the ground state $C0$, and first excited state $C1$. The valence-band states are assumed to be thermalized owing to the smallness of the level spacings relative to the conduction band. We begin by examining the transition rates between the trap state T and the two quantum dot states $C0$ and $C1$.

For either of the quantum dot states ($i = C0, C1$) the total energy is a sum of electronic and vibrational (thermal) energy:

$$V_i = E_i + \frac{1}{2}m\omega^2Q^2, \quad (1)$$

where it is assumed that the configuration of the interaction mode may be specified by a single coordinate Q . The total wave function is a product of an electronic and a vibrational wave function: $\psi_i(r, Q) = \varphi_i(r)\chi_i(Q)$. The electronic wave function for these conduction states is calculated using a single-band model in the effective-mass approximation.⁸ The potential energy V representing the band offset between the conduction bands of GaAs and $\text{In}_{0.5}\text{Ga}_{0.5}\text{As}$, has been calculated as 360 meV,⁹ for conditions of uniaxial strain. Solving for the energy of these states using material parameters given by Shur¹⁰ shows that $E_{C0} = 170$ meV and $E_{C1} = 332$ meV, as measured from the bottom of the $\text{In}_{0.5}\text{Ga}_{0.5}\text{As}$ conduction band.

For simplicity, we assume that the defect has only a single bound state. The Dirac δ function potential satisfies this criterion and we follow Sercel⁷ in using this potential to model the defect. The wave function is again a product of electronic and vibrational wave functions, with the electronic portion given by

$$\varphi_T = \sqrt{\frac{\alpha}{2\pi}} \frac{e^{-\alpha|\vec{r}-\vec{b}|}}{|\vec{r}-\vec{b}|}, \quad (2)$$

where $\alpha \equiv \sqrt{2m^*E_0/\hbar^2}$ is the wave number and \vec{b} is the distance from the center of the quantum dot to the defect. The electron-phonon coupling of the defect state is taken to be linear, so that the total energy of an electron in the trap takes the form of a displaced parabola

$$V_T = E_T + \frac{1}{2}m\omega^2(Q - Q_0)^2, \quad (3)$$

where $E_T \equiv E_0 - m\omega^2 Q_0^2/2$. It is helpful to introduce the Huang-Rhys factor S ,

$$S\hbar\omega = \frac{1}{2}m\omega^2 Q_0^2, \quad (4)$$

and the ‘‘number of phonons’’ p_l defined as the difference between the minima of the two energy curves corresponding to quantum dot state Cl and the defect state:

$$p_l\hbar\omega = E_{Cl} - E_T. \quad (5)$$

For comparison with the semiclassical rates derived previously,⁷ it is necessary to obtain an explicit formula for the coordinate of the crossing point as well as the height of the barrier between the two wells. These can be obtained from Eqs. (1) and (3):

$$Q_{Cl} = \sqrt{\frac{(S-p_l)^2\hbar}{2m\omega S}}, \quad EA_{Cl} = \frac{(S-p_l)^2\hbar\omega}{4S}. \quad (6)$$

The energy EA_{Cl} is measured from the bottom of the parabola which the electron occupies in its initial state. Figure 1 shows a configuration coordinate diagram depicting total-energy curves for both of the quantum dot states $C0$ and $C1$, the trap state T , as well as the quantities given in Eqs. (4)–(6).

Transitions between the dot and the defect fall into two different categories, depending on temperature. In the first case the thermal energy exceeds EA_{Cl} , the crossing point energy. This is the case that was treated by Sercel,⁷ and for which the semiclassical approach is valid. The second case is when the thermal energy in the system is less than EA_{Cl} . In that case the electron must tunnel through the barrier in configuration space in order to make a transition between the dot and the defect. In both of these cases ELECTRONIC tunneling occurs, since the dot and the defect are separated spatially. It is a second type of tunneling, through configuration space (nuclear tunneling), that is at issue in the low-temperature case. In this section we treat this second kind of tunneling using Fermi’s golden rule, which gives the transition rate *at a given energy* E in terms of a matrix element M , and the density of final states N_f :

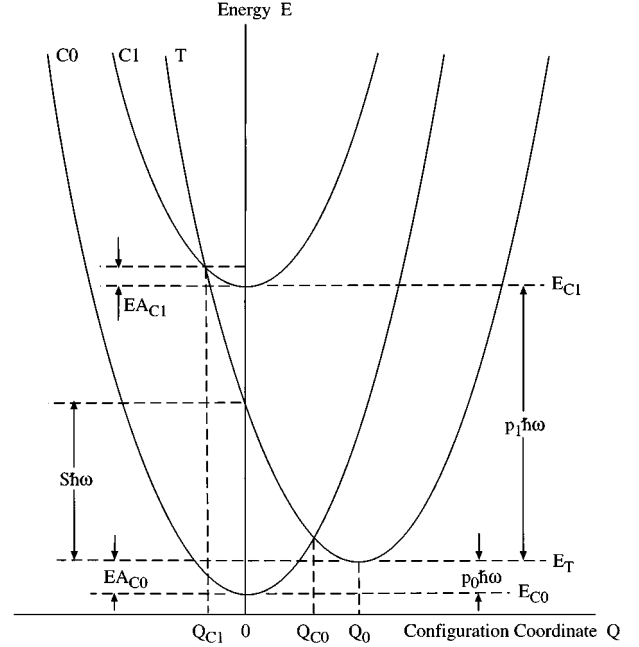


FIG. 1. Total-energy curves for the quantum dot states $C0$, $C1$, and the trap state T as a function of the configuration coordinate Q .

$$W(E) = \frac{2\pi}{\hbar} |M|^2 N_f. \quad (7)$$

The density of final states takes the form $1/\hbar\omega$,¹¹ so that the problem reduces to a calculation of the matrix element M .

The matrix element is the integral over the initial state, the Hamiltonian that causes the transition (the perturbation), and the final state:

$$M = \int_{-\infty}^{\infty} \int_{-\infty}^{\infty} \chi_i(Q)^* \varphi_i(r)^* H_{\text{int}}(r, Q) \chi_j(Q) \varphi_j(r) dr dQ. \quad (8)$$

Performing the integral over r gives the electronic matrix element $V(Q)$. Since the overlap of the vibrational components is sharply peaked at the crossing point Q_c ,¹¹ the electronic matrix element can be pulled outside of the integral:

$$M = V(Q_c) \int_{-\infty}^{\infty} \chi_i(Q)^* \chi_j(Q) dQ. \quad (9)$$

The integral in Eq. (9) is the overlap of two harmonic oscillator wave functions of arbitrary quantum numbers i and j , separated by a distance Q_0 . This integral can be calculated exactly, the result is

$$\left[\int_{-\infty}^{\infty} \chi_i(Q)^* \chi_j(Q) dQ \right]^2 = \frac{i!}{j!} \left(\frac{m^2 \omega^2 Q_0^2}{2\hbar^2} \right)^{j-i} e^{-m^2 \omega^2 Q_0^2 / 2\hbar^2} \left\{ L_i^{j-i} \left(\frac{m^2 \omega^2 Q_0^2}{2\hbar^2} \right) \right\}^2. \quad (10)$$

This gives us the rate for transitions out of a single state with energy E , $W(E)$; to obtain the more pertinent quantity, the total transition rate at a given temperature, we must perform a summation over all states, with each weighted by the appropriate

Boltzmann factor. This sum can be calculated exactly, and gives an equation for the transition rate at low temperatures with no approximations other than the ones latent in Fermi's golden rule. The result is

$$W(T) = \frac{2\pi |V(Q_c)|^2}{\hbar^2 \omega} \exp\left[-\text{Scoth}\left(\frac{\hbar\omega}{2kT}\right) + p \frac{\hbar\omega}{2kT}\right] I_p \left[\text{Scsch}\left(\frac{\hbar\omega}{2kT}\right) \right]. \quad (11)$$

In this equation, $p\hbar\omega$ denotes the ground-state energy difference between the defect and the relevant quantum dot state, defined in (5), while the Huang-Rhys parameter S , which characterizes the defect is defined in Eq. (4). As it stands this equation is extremely general. For example, the same result turns up in the study of electron transfer in biological systems.¹² It remains only to calculate the electronic matrix element $V(Q_c)$.

The electronic matrix element is calculated in the tight-binding approximation.⁸ This assumption is valid if the separation between the dot and defect is large enough. The total Hamiltonian may be written as

$$\hat{H} = \frac{\hat{p}^2}{2m^*} + V_{\text{TRAP}} + V_{\text{DOT}}, \quad (12)$$

where the first two terms together make up \hat{H}_{TRAP} , the Hamiltonian whose eigenstate is the defect wave function. The electronic matrix element can be written as

$$V(Q) = \langle \varphi_{\text{DOT}} | H_{\text{TRAP}} | \varphi_{\text{TRAP}} \rangle + \langle \varphi_{\text{DOT}} | V_{\text{DOT}} | \varphi_{\text{TRAP}} \rangle \\ = E \langle \varphi_{\text{DOT}} | \varphi_{\text{TRAP}} \rangle + \langle \varphi_{\text{DOT}} | V_{\text{DOT}} | \varphi_{\text{TRAP}} \rangle. \quad (13)$$

Since we are interested in the value of this matrix element at the crossing point $V(Q_c)$ where the energies of the two states are equal, the energy E in Eq. (13) can be taken to be the electronic energy of the quantum dot state involved in the transition. Figure 2 shows the electronic matrix element between the first excited state of the quantum dot and the defect

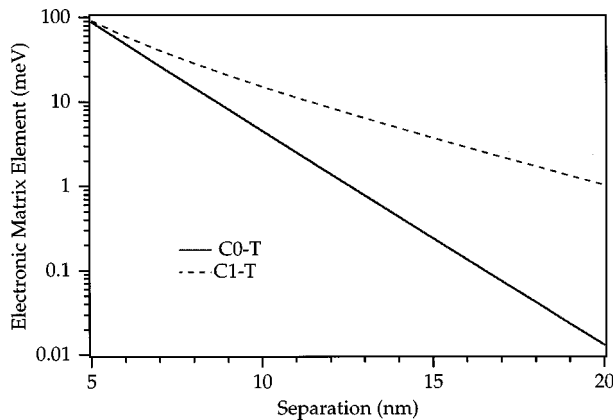


FIG. 2. Electronic matrix element $V(Q)$ for transitions between the defect and the ground quantum dot state (C0-T), and for transitions between the defect and the first excited quantum dot state (C1-T). Separation measures the distance between the defect and the center of the quantum dot. Parameters used are an effective electron mass $m^* = 0.041m_e$ and a band offset of $V = 360$ meV, giving rise to the bound-state energies $E_{C0} = 170$ meV and $E_{C1} = 332$ meV.

state (C1-T), and between the quantum dot ground state and the defect state (C0-T). These values, which are plotted as a function of separation between the quantum dot and the defect, were calculated numerically using the band-structure parameters chosen above.

Using the results of Fig. 2, we are able to calculate the total transition rate as a function of temperature. This is done for a separation of 10 nm in Fig. 3(a) and for a separation of 20 nm in Fig. 3(b). In order to perform this calculation a number of parameters must be specified. The Huang-Rhys factor S is chosen such that $S\hbar\omega = 100$ meV when the frequency ω is taken to be that of the TA phonon ($\hbar\omega = 10$ meV). The energy of the unoccupied trap is taken to be 275 meV. Therefore, for transitions from C1 to T the number of phonons $p = 16$, and for transitions from T to C0 it is 1. In order to obtain the transition rates for the opposite direction, the sign of p is reversed. These are values typical of the electron trap M1 common to GaAs grown by molecular-beam epitaxy.^{13,14}

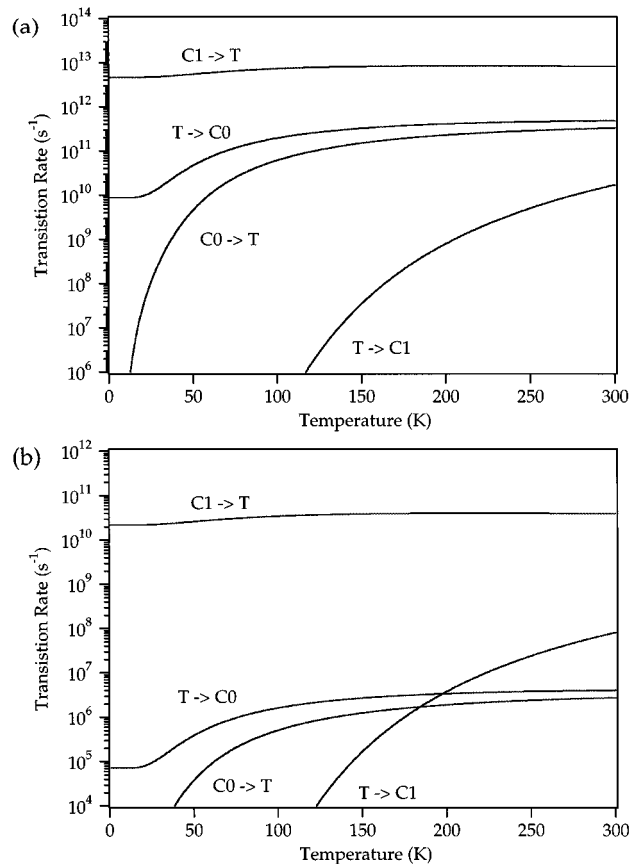


FIG. 3. Total transition rates between the quantum dot and the defect at (a) a dot-defect separation of 10 nm and (b) a dot-defect separation of 20 nm. Parameters used are $S = 10$, $\hbar\omega = 10$ meV, $p_0 = 1$, and $p_1 = 16$.

Figure 3(a) shows that for a dot-defect separation of 10 nm the rate $C1 \rightarrow T$ is on the order of 10^{13} s^{-1} , and the rate $T \rightarrow C0$ is on the order of 10^{10} s^{-1} , at 0 K. The reverse rates are in fact “frozen out” at low temperatures, since such transitions would require an influx of energy into the system. If the distance between the dot and the defect is increased to 20 nm, a substantial reduction is seen in the transition rates [Fig. 3(b)]. The fact that the T to $C0$ rate drops to approximately 10^5 s^{-1} means that the defect-assisted tunneling mechanism would not serve to overcome the “phonon bottleneck” at such a large separation.

In this work we have modeled the effect of coupling to a deep-level trap on electron relaxation in quantum dots in the low-temperature limit. The main conclusion of the present analysis is that the presence of point defects may serve to *enhance* the luminescence efficiency of quantum dot material, even at low temperature, a regime in which defect-related processes might have been expected to be frozen out. The persistence of the defect relaxation process at low tem-

perature is due to tunneling through the defect activation barrier for capture and emission. As discussed in Ref. 7, the physical situation described in this paper could only arise if the spatial distribution of defects is strongly correlated with that of the quantum dot structures, e.g., through formation of interface states or point defects as a consequence of the growth process. That this situation commonly exists in MBE-grown material is demonstrated, for example, by the observation of resonant enhancement of nonradiative processes involving point growth defects in MBE-grown $\text{Al}_x\text{Ga}_{1-x}\text{As}/\text{GaAs}$ quantum wells.¹⁵ With this caveat, the proposed mechanism may thus explain the failure to observe a significant phonon bottleneck effect in recent work on $\text{In}_x\text{Ga}_{1-x}\text{As}$ quantum dot structures.

This material is based upon work supported by the National Science Foundation under Grant No. DMR 9304537. Support by the Oregon Joint Centers for Graduate Schools in Engineering is gratefully acknowledged.

*Present address: Department of Physics, 117 Clark Hall, Cornell University, Ithaca, NY 14853-2501.

¹U. Bockelmann and G. Bastard, *Phys. Rev. B* **42**, 8947 (1990).

²H. Benisty, C.M. Sotomayor-Torres, and C. Weisbuch, *Phys. Rev. B* **44**, 10 945 (1991).

³G. Wang, S. Fafard, D. Leonard, J.E. Bowers, J.L. Merz, and P.M. Petroff, *Appl. Phys. Lett.* **64**, 2815 (1994).

⁴T. Inoshita and H. Sakaki, *Phys. Rev. B* **46**, 7260 (1992).

⁵U. Bockelmann and T. Egeler, *Phys. Rev.* **46**, 15 574 (1992).

⁶A.I. Efros, V.A. Kharchenko, and M. Rosen, *Solid State Commun.* **93**, 281 (1995).

⁷Peter C. Sercel, *Phys. Rev. B* **51**, 14 532 (1995).

⁸Peter C. Sercel and Kerry J. Vahala, *Phys. Rev. B* **42**, 3690 (1990).

⁹X. Marie, J. Barrau, B. Brousseau, Th. Amand, M. Brousseau, E.V.K. Rao, and F. Alexandre, *J. Appl. Phys.* **69**, 812 (1991).

¹⁰Michael Shur, *Physics of Semiconductor Devices* (Prentice-Hall, Englewood Cliffs, NJ, 1990).

¹¹T. Markvart, in *Recombination in Semiconductors*, edited by P.T. Landsberg (Cambridge University Press, Cambridge, 1991), Chap. 6.

¹²Christopher C. Moser, Jonathon M. Keske, Kurt Warncke, Ramy S. Farid, and P. Leslie Dutton, *Nature* **355**, 796 (1992).

¹³D.V. Lang, A.Y. Cho, A.C. Gossard, M. Ilegems, and W. Weigman, *J. Appl. Phys.* **47**, 2558 (1976).

¹⁴P. Blood and J.J. Harris, *J. Appl. Phys.* **56**, 993 (1984).

¹⁵A. Fujiwara, K. Muraki, S. Fukatsu, Y. Shiraki, and R. Ito, *Phys. Rev. B* **51**, 14 324 (1995).